



Research Article

Effect of various reactor temperatures for mixed metallic oxides in chemical looping combustion system for carbon capture

Mit Manojbhai SHETH¹, Atal Bihari HARICHANDAN², Rameshkumar BHORANIYA^{1,*}

¹Department of Mechanical Engineering, Marwadi University, Gujarat, 360 003, India

²Department of Mechanical Engineering, Biju Patnaik University of Technology, Odisha, 769015, India

ARTICLE INFO

Article history

Received: 10 April 2024

Revised: 24 July 2024

Accepted: 26 July 2024

Keywords:

Bubble Hydrodynamics; Carbon Capture; Chemical Looping Combustion; Mixed Metal Oxides; Operating Temperature

ABSTRACT

Chemical looping combustion (CLC) is an innovative technology designed to address the growing concerns related to carbon dioxide (CO₂) emissions from fossil fuel-based power plants. As the world grapples with the challenges of climate change, the development of efficient and cost-effective carbon capture technologies has become imperative. CLC emerges as a promising solution, offering a unique approach to capturing CO₂ while maintaining energy efficiency in power generation. The study of bubble hydrodynamics within the fuel reactor of a CH₄-fueled CLC system has been incorporated into the present research work. The reaction kinetics have been incorporated into the reactive system of the fuel reactor by a user-defined function (UDF) during numerical analysis. The present study uses CuO and NiO as mixed oxygen carrier materials in various proportions and CH₄ as a fuel in combustion processes. The various proportions of mixed metallic oxides have been considered as 30% CuO and 70% NiO, 50% CuO and 50% NiO, and 70% CuO and 30% NiO by volume. The bubble hydrodynamics in terms of development, growth, rise, and burst are visualized and analyzed in the solid-gas molar fraction inside the fuel reactor. In the recent work, authors have chosen different operating temperatures varying from 923 K to 1323 K. The fuel conversion rate has been observed to increase with the increased temperature.

Cite this article as: Sheth MM, Harichandan AB, Bhoraniya R. Effect of various reactor temperatures for mixed metallic oxides in chemical looping combustion system for carbon capture. J Ther Eng 2025;11(3):716–726.

INTRODUCTION

The global energy landscape is evolving at an unprecedented rate, driven by a growing population, increasing energy demands, and the imperative to mitigate the adverse effects of greenhouse gas emissions on the environment. In this context, the search for cleaner and more efficient

energy conversion technologies has gained paramount importance. One promising approach is CLC, the novel and innovative combustion system that has the potential to significantly reduce the emissions of carbon dioxide (CO₂) while efficiently utilizing a variety of fuels, including gaseous fuels such as natural gas and hydrogen [1-3].

*Corresponding author.

*E-mail address: rameshbhoraniya@gmail.com

This paper was recommended for publication in revised form by Editor-in-Chief Ahmet Selim Dalkılıç



Traditional combustion processes, such as coal and gas combustion, have been the primary sources of energy production for decades. However, their reliance on direct contact between fuel and oxygen in the air results in production of CO₂ and other pollutants. Over the past few decades, the issue of global climate change and its impact on society has been a central focus of research for various scientific communities. The emission of greenhouse gases such as CO₂, NO_x, and SO_x play a significant role in global climate change, with CO₂ leading the way among these contributors. The burning of non-renewable energy sources for energy production has been a cornerstone related to human progress for centuries, but it has come at a significant cost to the environment due to the emission of CO₂ and other pollutants. This has led to the exploration of new pathways to meet energy demands without exacerbating climate change. CLC has emerged as a promising solution by offering the possibility of efficient energy conversion while capturing CO₂ before it is released into the atmosphere [4]. Many scientists have noted that a significant portion of carbon dioxide releases results from the burning of non-renewable energy sources, and in the present era, over one-third of total carbon dioxide releases originate from fuel combustion. A pressing challenge of mitigating CO₂ emissions requires transformative approaches that have led to exploration related to carbon capture and storage (CCS) technologies by means to capture and isolate CO₂ emissions. CLC presents a unique approach to CCS by enabling the capture of CO₂ during the combustion process itself, eliminating the need for costly and energy-intensive separation steps. CLC offers an alternative approach by using a solid oxygen carrier to facilitate the combustion process, allowing for the separation of oxygen from air and fuel streams. This inherent separation leads to several advantages, including increased energy efficiency and a reduced environmental footprint [5, 6].

While CLC has garnered attention for its potential to reduce CO₂ emissions, its application with gaseous fuels represents a critical area of research. Gaseous fuels, such as natural gas and hydrogen, are abundant and possess high energy densities. In recent decades, hydrogen (H₂) has gained recognition as an environmentally friendly fuel on Earth and a sensible substitute for fossil fuels, as it generates only water without any greenhouse gas emissions. There are claims that hydrogen will be utilized as an energy transporter in a variety of energy systems in the coming years [7].

There would be two interconnected reactors namely the air reactor and fuel reactor; where the reduction process takes place in the fuel reactor and oxidation in the air reactor solid particles as shown in Figure 1. The core chemistry of CLC involves two main redox reactions: the process of oxygen carrier oxidation within AR and its subsequent reduction within FR. In an air reactor, an oxygen carrier releases oxygen upon contact with air, facilitating combustion of fuel. The O₂ transporter in its reduced state

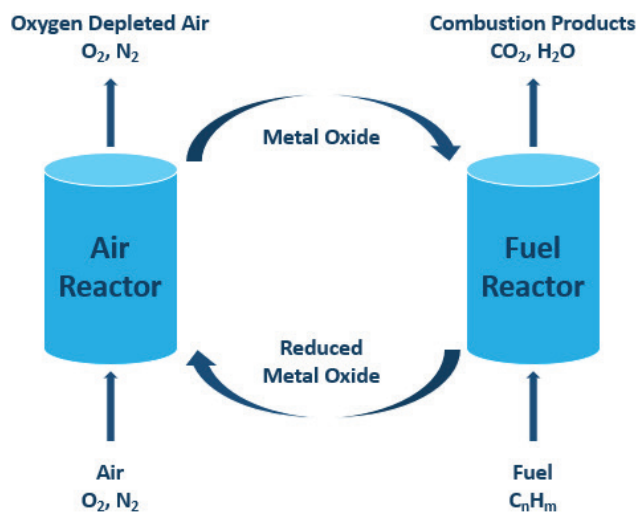
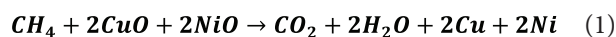


Figure 1. CLC system diagram.

then transfers within FR, in which it captures oxygen from fuel. This process creates a loop in which the oxygen carrier continuously cycles between oxidized and reduced states. CLC systems commonly employ dual FBR – one for AR and one for FR. Fluidization involves suspending solid particles in a gas stream, creating a bed with properties resembling that of a fluid. In AR, the O₂ transporter bed has been fluidized using air, allowing for efficient oxygen uptake. The fuel reactor operates in a similar manner, where the bed of reduced oxygen carrier interacts with the fuel stream. Using dual fluidized beds ensures the separation of air and fuel streams, preventing direct mixing and enabling efficient oxygen transfer. CLC offers substantial CO₂ mitigation potential by capturing CO₂ during the combustion process. This not only reduces direct emissions but also simplifies the subsequent capture and storage steps. The reduced emissions of nitrogen oxides and other air pollutants make CLC a promising technology for improving air quality and minimizing the environmental impacts of combustion processes. While CLC reduces CO₂ emissions, it is essential to consider potential impacts on water and resource usage. The extraction, processing, and disposal of oxygen carriers and other materials must be evaluated from a life cycle perspective.

The chemical reactions of hydrocarbon fuel and mixed metal oxides in the fuel reactor is given below:



Ishida et al. [1] employed a graphic exergy study to evaluate the power production abilities of a Chemical Looping Combustion process. The exergy analysis of power generation systems often relies on energy utilization diagrams. One key observation is that as exergy losses decrease, the overall efficiency of a power plant improves. Achieving this entails generating power using gas turbines operating at higher

temperatures and conducting burning processes at higher temperatures, which can substantially reduce exergy losses within the combustor. By implementing CLC, it's possible to enhance thermal efficiency by as much as 50.2%. Lackner et al. [2] proposed a concept for a burning engine that employs numerous FBRs based on principles related to CLC. A reactivity of solid particles was assumed and subsequently verified. In this system, solid fuels are used as the primary source of fuel and natural gas can be employed within the CLC technique. Lyngfelt et al. [3] introduced a combustor design that comes from the principles of the CLC system. This design incorporates dual linked fluidized chambers: low-momentum bed & high-momentum riser. To ensure the viability of the system, a reactive nature of the metallic oxide elements was initially hypothesized; and subsequently confirmed through data found from publicly accessible sources. While CLC typically employs gasified solid fuels as the primary energy source, it is worth noting that fossil gas can also be readily utilized directly within the CLC system. Hossain and de Lasa [4] investigated CLC as a leading innovation on the side of burning fossil fuels & CO₂ mitigation. They proposed a setup comprising two linked fluidized bed reactors, with the O₂ transporter flowing back and forth amongst both reactors. This setup offers a practical solution for capturing and separating CO₂ through the exhaust gases generated during the burning of fossil fuel, potentially reducing emissions related to primary gases. The focus of this study was to identify suitable oxygen carriers for power generation using CLC. Dahl et al. [5] introduced a novel reactor concept designed for a CLC system fueled by natural gas. This innovative reactor takes the form of a rotating system with a fixed bed containing metal oxide particles, which are rotated between the zones where CH₄ (methane) and air are introduced. To prevent uncontrolled mixing of CH₄ and air, an inert gas is introduced into the mixture zone of CH₄ and air. The study focused on the use of CuO/Al₂O₃-based metal oxide particles and discussed the rationale behind selecting this combination for analysis. Kruggel-Emden et al. [6] performed trial investigations about kinematic prototypes related to CLC. Their findings suggest the models based on observations and data, and they recommended the adoption of these empirical models to enhance large-scale simulations. Additionally, they developed a dual-component experimental calculation grounded upon a rate of reaction derived from a kinematic prototype. Cho et al. [7] conducted experiments under steady-state conditions, resulting in the conversion of 94.15% of CH₄ into CO₂ and the production of 99.95% of H₂. These experiments were carried out using a continuous 300 W TRCL testing plant. In the continuous operation of this plant, FeO₂ has been effectively abridged into FeO within FR through the utilization of methane as gaseous reduction. Subsequently, the abridged elements underwent oxidation through a reaction between steam & iron occurring within SR. Notably, the rate of production related to H₂ achieved in this process reached 63% of the theoretical limit. Harichandan and Shamim [8] conducted a detailed computational fluid

dynamics investigation related to air pocket dynamics within FR of H₂ fired CLC process. The primary focus of this study was to examine dynamic behavior related to bubbles within FR over time, employing a CFD approach. The CFD tool also enabled the simulation of solid and gaseous phase mole fractions of the resulting products. The research revealed that bubble hydrodynamics were prominently observed during the initial 1.6 seconds. After this period, a coral-like structure emerged, representing a mixture of solid & gas elements, ultimately reaching a near-equilibrium state. The study assessed rates of fuel transformation under various conditions. Harichandan and Shamim [9] conducted a study investigating hydrodynamics related to FR within the CLC technique. They employed multiple phases 2D computational fluid dynamics prototype which incorporated all interactions and reactions chemically between gases and solids. The research involved a comparative analysis of two CLC systems, each utilizing a different fuel and oxygen carrier. Specifically, hydrogen (H₂) was used with CaSO₄, while methane (CH₄) was employed with NiO. The study revealed distinctive features in the behavior of gaseous bubbles, including their generation, growth, rise, and bursting, which were more pronounced within a reactor powered by H₂ fuel in contrast to a reactor powered by CH₄. Furthermore, it has been noted that the rate of conversion related to fuel increased along with higher operating temperatures. The CH₄-fueled and H₂-fueled reactors operated at temperatures of 950 K and 1150 K, respectively. To achieve a high fuel conversion rate, the study considered relatively narrow bed widths and the use of nano-sized metal oxide particles. Niu et al. [10] conducted an investigation into the burning efficiency of wastewater treatment residue using a continuous CLC system having hematite as OC. The results revealed that sewage sludge exhibited remarkable combustion efficiency, even on a comparatively reduced temperature of 800 °C, making it a distinctive solid fuel. Importantly, during the CLC of sewage sludge, no elements of char had been observed bypassing to AR. Larring et al. [11] conducted research focused on various mineral samples that exhibited the unique property of not requiring any activation or pre-processing, including thermal treatment. They conducted experiments utilizing Thermogravimetric Analysis (TGA) and obtained back-scattered electron images of minerals. Nonetheless undergoing beginning at approximately 900 to 950°C, it was observed that Kryvbas and Sinai-A ores displayed a superior capacity for oxygen transport compared to Ilmenite. Additionally, manganese (Mn) and iron (Fe) based combined oxide particles exhibited minimal separation and particle swelling on the surface during reaction cycles. As a result, they demonstrated that there was no need for pre-processing when utilized in Chemical Looping Combustion (CLC) processes. Khan and Shamim [12] conducted a thermodynamic evaluation of appropriate OCs for TRCLR. This screening was based on various criteria, including physical/chemical properties & O₂ partial pressure. The authors created multiple reaction pathways and calculated the associated Gibbs free

energies & enthalpies of reaction. After a screening process, the last selected paths of reactions included materials based on Fe, Mo, V, and W. Notably, Fe and Mo based OCs were found to effectively completely burn CH_4 within Fuel Reactor on less than 800 K temperature, whereas O_2 transporter based on tungsten and vanadium needed temperatures higher than 1200 K. Yaoyao et al. [13] successfully produced hydrogen-rich gaseous generated through methane at 673 K using a one-stage procedure, void of a distinct O_2 source. The innovative approach has been implemented in a reactor with a packed bed assisted by plasma with nickel-related catalysts with added dopants onto a supportive material that is reactive. Amongst all various elements tested, nickel or iron oxides exhibited remarkable promise. Its exceptional catalytic performance appeared to be attributed to the presence of Fe_2O_3 , which effectively curtailed carbon deposition. Sedghkerdar et al. [14] performed research to evaluate viability related to CLC utilizing solidus fuel. They employed a newly created O_2 transporter composed of nickel and reinforced by a zirconia-coated gamma-alumina shell within thermogravimetric analyzer. To understand the reaction rates of reduction and oxidation in the CLC process with solidus fuel, researchers devised a model related to GSDM by forecasting the initial distribution of grain sizes., taking into account the “pore to sphere” factor. Pragadeesh et al. [15] investigated the transformation of sizable fuel particle’s char & the phenomenon related to fragmentation of char fragmentation within the inset gasification Chemical Looping Combustion (CLC) environment. They conducted experiments using three distinct types of coal and wood-derived biomass particles ranging from a size of more than 8 mm to 25 mm at three distinct bed temperatures in a batch reactor utilizing a hematite CLC system, employing steam as an agent for fluidization or gasification. Jovanovic and Marek [16] introduce a novel modeling approach applied to the reduction of hematite to magnetite - a predominant reaction in environments featuring a high CO_2/CO ratio, as anticipated in chemical looping combustion processes. The Fe_2O_3 particle’s structure was replicated using percolation theory, while the reduction process was simulated using a stochastic approach encompassing nucleation, gaseous diffusion, solid-state diffusion, and chemical reactions. This model offers valuable insights into the intricacies of the studied process. Liu et al. [17] provide an overview of how density functional theory (DFT) contributes to our understanding of the mechanisms involved in the generation of O_2 transporters related to the CLC technique. They summarize the responsiveness of oxygen-carrying materials and delve into intricate details of reaction mechanisms. The review also sheds light on the interactions between different components and the synergistic effects within oxygen carriers. Yamamoto et al. [18] performed research on methanation reactivity using chemical equilibrium calculations. They explored the impact of altering ambient pressure, response temperature, and the proportion of carbon dioxide to H_2 . Major findings indicated that a transformation of CH_4 reached 100% whereas the Hydrogen

to CO_2 Ratio was less than 1 in the absence of oxygen. Song et al. [19] developed a machine-learning model capable of predicting the impact of various factors. They assembled records containing 190 tasters for training both SVM & BP-ANN algorithms. Based on the replica’s predictions, copper-bearing minerals were anticipated to exhibit exceptional effectiveness of reaction, with approximately 68% CH_4 transformation & 96% transformation of CO on 950 °C. Sheth et al. [20] indicated the performance of fuel reactor in CLC system by considering NiO and CuO as separate metallic oxides. The unsteady bubble hydrodynamics of fuel reactor, solidus volume fraction and fuel conversion rate has been shown in the literature. Due to improper mixing of fuel and metal oxide particles, the fuel conversion rate was found lower. They suggested that the conversion of fuel has been increased with increase of temperature. Sheth et al. [21] performed analysis of fuel reactor considering various sizes metal oxide particles ranging from 100 μm to 400 μm and various operating temperatures ranging from 923 K to 1223 K. It has been suggested that the fuel conversion take place higher while operating with high temperature. The rate of fuel conversion has been found to increase for nano-size particles. Sheth et al. [22] performed the numerical analysis of fuel reactor considering CuO and NiO as mixed metal oxides and CH_4 as fuel. They concluded that the rate of fuel conversion if high while CuO content is more in mixed oxides proportions because of the better reactivity of CuO at high temperature. Mahalatkar et al. [23] have analyzed a CLC system, which includes fuel burning through chemical reactions involving an O_2 transporter exchanged between two reactors, which is described in the work using CFD. This research is related to FR. When a simulation’s output is compared to in-depth experimental data, it is discovered that the results are reasonably accurate. The study advances knowledge of the CLC process and emphasizes the usefulness of CFD simulations in this field. Arjmand et al. [24] presented a brief exploring a potential of modeling viable O_2 transporter elements through combinations of various oxides. Their investigation combined both experimental work on TGA and thermodynamic considerations for assessing a feasibility related to these materials. Reactivity data obtained from experimental studies indicated that these systems exhibited a high rate of O_2 release, making them suitable for practical applications. Furthermore, it was observed that manganese ions offered a wide range of oxidation states, allowing for the creation of numerous combined oxides. Vega et al. [25] sought to enhance the interaction between gases and solids within FR through introducing internals in the shape of rings. They conducted two sets of experiments in CLC with a thermal capacity of 50 kW, where a type of soft coal was combusted alongside elements made of ilmenite within temperatures ranging from 900 to 1000 °C. The utilization of these internals resulted in a 20% reduction in total oxygen demand, decreasing from 12.2% to 9.8%. Adanez et al. [26] macroscopic models have proven macroscopic models effectiveness in accurately predicting the fluid dynamics within large fluidized bed reactors. They presented

a vertical solids profile that closely matched experimental data obtained from 226 MW circulating fluidized beds. Jung and Gamwo [27] utilized a fluidized bed that circulates in their CLC process, which included a dual reactor system and a compatible metal oxygen carrier. The physical modeling of the reactors did not incorporate any groundbreaking technologies or high-risk elements. Khongprom and Gidaspow [28] applied Multiple-phase CFD techniques to create a small FBR sorbent system for extracting carbon dioxide from fuel gases, employing potassium/sodium carbonate pills. Their modifications to an absorber's dimensions effectively eliminated the presence of dilute regions responsible for system bypassing. Additionally, they successfully eliminated the core annular regime by implementing appropriate solid configurations. Xiao and Song [29] conducted a numerical investigation using CaSO_4 as metallic oxide in their study. They used computational fluid dynamics (CFD) analysis to describe bubblic generation & its impact on concentration in the gas phase. Their findings indicated that the rate on which fuel is converted; was reduced because of the rapid & extensive formation of bubbles, the large size of elements & low bed temperatures. Snider et al. [30] CFD was effectively employed to simulate the entire loop, encompassing AR, cyclone, and FR, in a scaled-down cold-flow system. Gayan et al. [31] discussed a performance related to O_2 carrier depends upon Al & Cu at elevated temperatures. They conducted experiments considering the O_2 transporter depends on Cu having methane as fuel, maintaining maximum operating temperatures of 1173 K for FR & 1223 K for AR. Their findings suggest that minimizing contact could be beneficial as the temperature resistance of metal oxide increases. Rajak et al. [32] uses CFD and the standard $k-\epsilon$ turbulence model to investigate how thermal radiation affects the simulation of turbulent, non-premixed combustion for different fuel-air combinations in a 2D cylindrical chamber. The results indicate that whereas kerosene-air has superior emission properties, hydrogen-air fuel generates the highest NO emissions. Because hydrogen-air burns more efficiently, it also produces less CO_2 emissions. There was a noticeable drop in the emissions of NO, H_2O , and O_2 .

In the present work, computational fluid dynamics has been used to model the fuel reactor of CLC process. Nevertheless, limited contributions have been described in the literature on the use of the CFD as a tool in the simulation of the CLC process. It is considered the nonlinear behavior of Cooper oxide, Nickle oxide, and methane as reactants and carbon dioxide, water vapor, copper, and nickel as a product. As an objective, it analyzes unsteady bubble hydrodynamics of FR in the CLC process by considering methane as fuel and copper oxide and nickel oxide as oxygen transporter to analyze the effect of different temperatures on the behavior of the chemical looping combustion process. Due to the higher oxygen transfer capacity and better reaction kinetics, authors have selected copper and nickel-based oxygen carriers for study.

MATHEMATICAL MODELING

The specific hydrodynamic equations resolved for unsteady and isothermal fluid-solid interactions within each phase are outlined below:

Continuity Equation

For phase j:

$$\frac{\partial}{\partial t}(\alpha_j \rho_j) + \nabla \cdot (\alpha_j \rho_j \vec{v}_j) = \sum_{a=1}^n (\dot{m}_{ij} - \dot{m}_{ji}) + S_j \quad (2)$$

where ρ_j is density and \vec{v}_j is velocity for phase j and \dot{m}_{ij} represents the transfer of mass originating from i^{th} to j^{th} stage, \dot{m}_{ji} represents the transfer of mass originating from j to phase i. S_j represents a source terminology. The exchange of mass, momentum, and energy between gas and solid phases is taken into account to analyze the continuity equation:

Momentum Equations

For phase j:

$$\frac{\partial}{\partial t}(\alpha_j \rho_j \vec{v}_j) + \nabla \cdot (\alpha_j \rho_j \vec{v}_j \vec{v}_j) = -\alpha_j \nabla i + \nabla \cdot \vec{\tau}_j + \alpha_j \rho_j \vec{g} + \sum_{a=1}^n (\vec{R}_{ij} + \dot{m}_{ij} \vec{v}_{ij} - \dot{m}_{ji} \vec{v}_{ji}) + (\vec{F}_j) \quad (3)$$

\vec{F}_j is body force consisting of virtual mass, lift, and force involved in interface amongst both stages. \vec{v}_{ij} is internal phase velocity. If $\dot{m}_{ij} > 0$ (i.e., Mass from phase i is being conveyed to phase j.), $\vec{v}_{ij} = \vec{v}_j$; if $\dot{m}_{ij} < 0$ (i.e., Mass from phase j is being conveyed to phase i.), $\vec{v}_{ij} = \vec{v}_i$. Similarly, if $\dot{m}_{ji} > 0$ then $\vec{v}_{ji} = \vec{v}_j$ if $\dot{m}_{ji} < 0$ then $\vec{v}_{ji} = \vec{v}_i$. \vec{R}_{ij} depends on the cohesion, friction, pressure, and additional influences, and is subject to circumstances that $\vec{R}_{ij} = \vec{R}_{ji}$ and $\vec{R}_{jj} = 0$. Within multiphase flows, particles experience lift forces ($\vec{F}_{lift,j}$) stemming from velocity gradients in the primary phase (gas) flow. These forces become more prominent with larger particles. However, our current model assumes particle diameters significantly smaller than inter-particle spacing. Consequently, accounting for lift forces becomes inappropriate for densely packed or extremely small particles.

Species Transport Equations

The conservation equations governing chemical species within multiphase flows for each phase k forecast the local mass fraction of each species, Y_m^n via solving a convection-diffusion equation corresponding to m^{th} species. When adapted to the multiphase blend, the comprehensive chemical species conservation equation can be expressed in the subsequent manner:

$$\frac{\partial}{\partial t}(\rho^j \alpha^j Y_m^j) + \nabla \cdot (\rho^j \alpha^j \vec{v}^j Y_m^j) = -\nabla \cdot \alpha^j \vec{J}_m^j + \alpha^j R_m^j + \alpha^j S_m^j + \sum_{a=1}^n (\dot{m}_{im}^j - \dot{m}_{jm}^i) + \mathfrak{R} \quad (4)$$

$$\frac{\partial}{\partial t}(\rho^j \alpha^j Y_m^j) + \nabla \cdot (\rho^j \alpha^j \vec{v}^j Y_m^j) = -\nabla \cdot \alpha^j \vec{j}_m^j + \alpha^j R_m^j + \alpha^j S_m^j + \sum_{\alpha=1}^n (\dot{m}_{i m j n} - \dot{m}_{j n i m}) + \mathfrak{R} \quad (5)$$

here, R_m^j denotes the overall rate at which homogeneous species m is generated through chemical reactions within phase j , $\dot{m}_{j n i m}$ represents the source of mass transport between species m and n , moving from phase j to phase i , and \mathfrak{R} signifies a rate of heterogeneous reactions. Furthermore, α^j represents the volume fraction pertaining to phase j and S_m^j stands for creation rate of additional material originating from the dispersed phase along with any sources defined by users. \vec{j}_m^j represents the diffusive flux resulting from temperature and concentration variances. The dilute approximation technique, following Fick's Law, is employed to study mass diffusion due to variations in concentration.

Figure 2 demonstrates the arrangement and computational grid employed in the CLC process. Initially, the Fluidized Bed Reactor (FBR) contained solid particles up to 40% of its stationary bed height. A total volume fraction of 0.48 for solid particles was distributed within the stationary bed height [33]. To avoid particle spacing from reaching zero, the maximum particle packing $\epsilon_{s,max} = 0.6$. The reactor's computational domain was discretized into 2500 rectangular cells and therefore, no grid independence test is required [34].

RESULTS AND DISCUSSION

The three various proportions of mixed metallic oxides have been considered as (i) NiO 0.7 and CuO 0.3 by weightage, (ii) NiO 0.5 and CuO 0.5 by weightage, and (iii) NiO 0.3 and CuO 0.7 by weightage for the study. The impact of varying reactor temperatures on different ratios of CuO

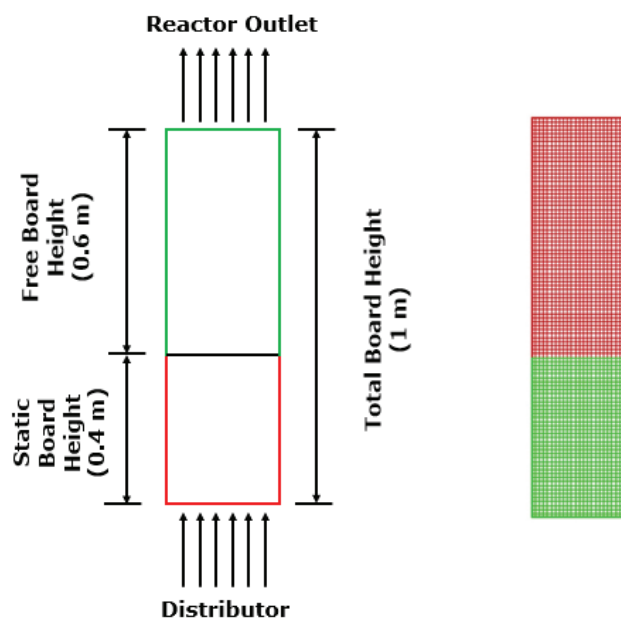


Figure 2. Fuel reactor layout with computational grids.

and NiO mixed metal oxides has been investigated for the fuel reactor in the Chemical Looping Combustion (CLC) system. This study aims to optimize the reactor's performance by understanding how temperature influences the reactivity and efficiency of the metal oxide mixtures [35].

An unsteady perturbation of the fraction of mole for gas reactant (CH_4) at interface and reactor outlet at different reactor inlet temperatures of the fuel reactor are presented in Figure 3 (a) and 3 (b) respectively. A simulation was carried out for NiO 0.7 as well as CuO 0.3 by weightage for various temperature ranges: 923 - 1223 K. The fluctuation of gaseous mole fraction within the fuel reactor has been

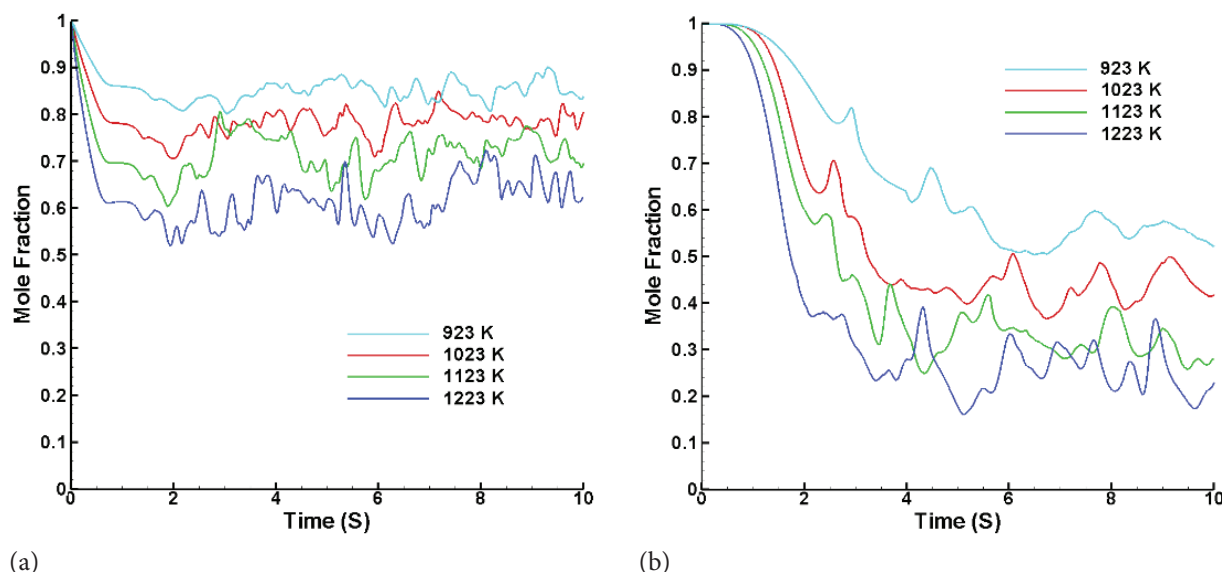


Figure 3. Molar fraction of reactant (CH_4) in (a) intersection and (b) outside for 30% CuO and 70% NiO.

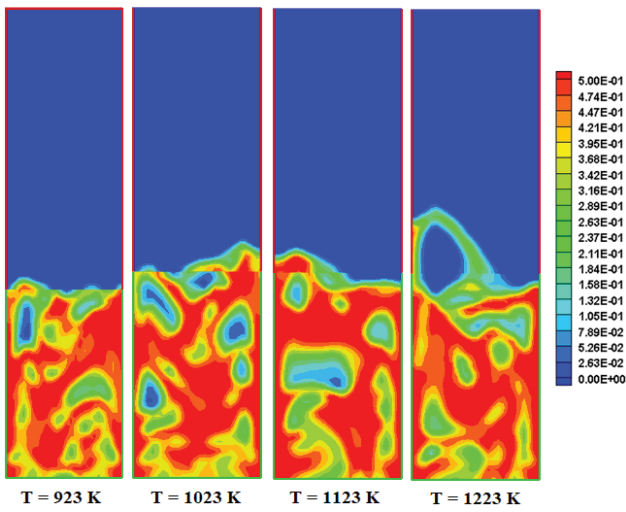
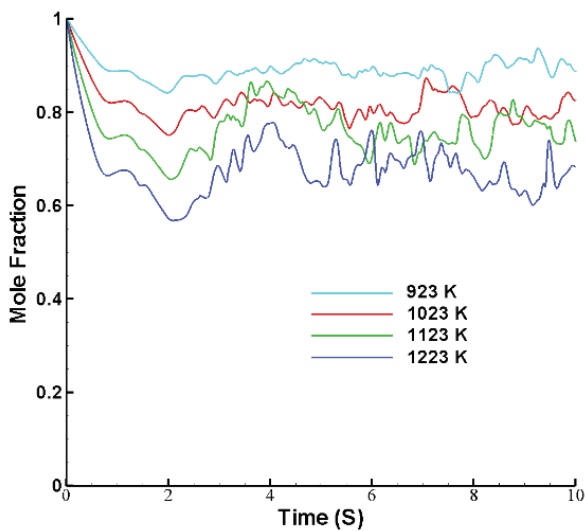


Figure 4. Solid volume fraction contour for various temperatures at time 10 s for 30% CuO and 70% NiO.

noticed to be more intense at higher temperature ranges. The fraction of mole related to CH_4 in the intersection has been observed to reduce gradually up to $t = 2$ s from unity. However, they fluctuate in a very irregular pattern beyond $t = 2$ s for all the temperature ranges under consideration. While the average molar fraction variation of CH_4 at outlet decreases progressively up to $t = 4$ s for a reactor inlet temperature of 1223 K to $t = 6$ s for a reactor inlet temperature of 923 K.

Beyond that, a quasi-steady distribution of mole fraction has been observed. This almost periodic variation of CH_4 mole fraction at outlet might result from the lack of particles carrying O_2 and less intense reactions.



(a)

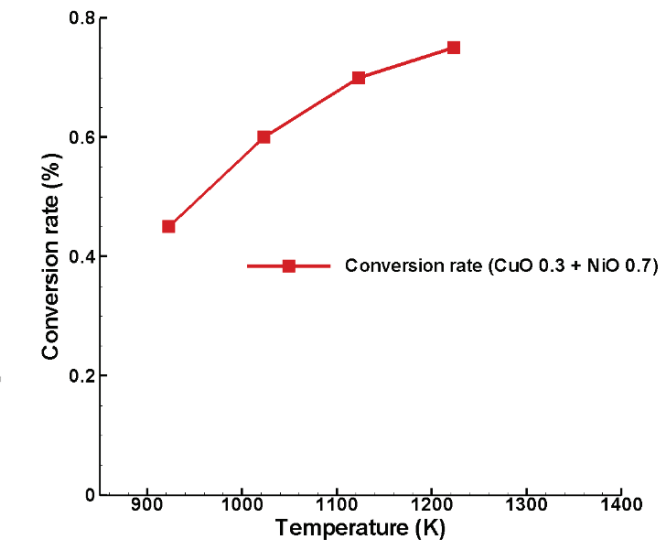
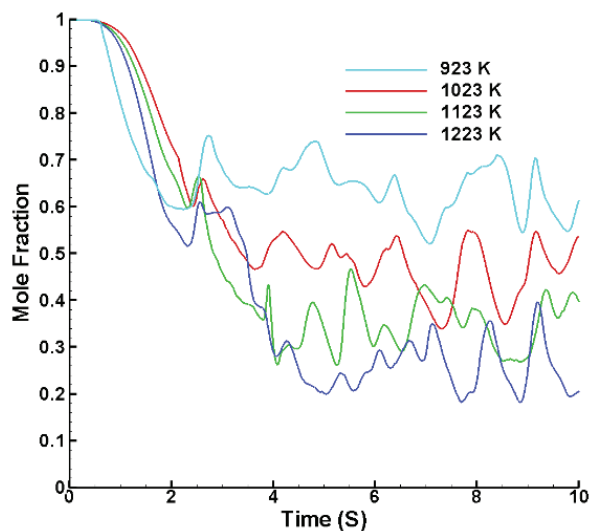


Figure 5. Conversion rates of fuel at outlet for different temperature ranges for 30% CuO and 70% NiO.

A contour displaying solidus volume portion considering different temperature spans, ranging from 923 - 1323 K, in time 10 seconds, is presented in Figure 4. It has been observed that at higher temperatures, the O_2 transporter molecules are thoroughly blended within the gas phase fuel particles, while in comparatively lower inlet temperatures, a significant amount of metal oxide granules is still discernible within FR. Consequently, this results in a reduced rate of inter-mixing between gas and solid molecules at lower temperatures, leading to low response rates.

Figure 5 illustrates the rate of conversion of fuel in outside for different temperature series. It's discerned that the effective blending of gas and solidus elements takes place in



(b)

Figure 6. Molar fraction of reactant (CH_4) in (a) intersection and (b) outside for 50% CuO and 50% NiO.

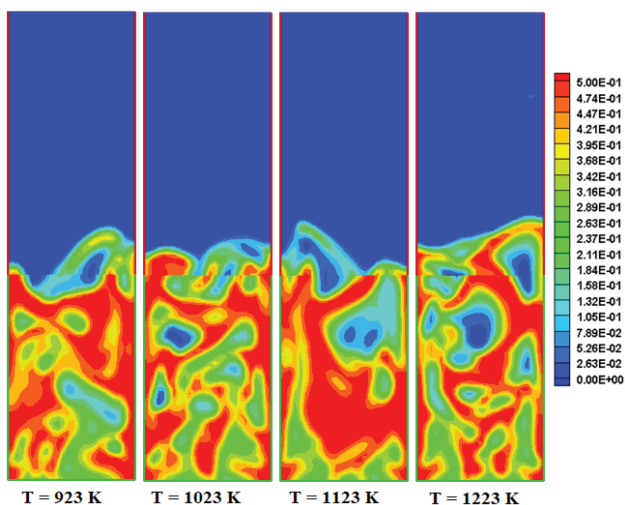


Figure 7. Solid volume fraction contour for various temperatures at time 10 s for 50% CuO and 50% NiO.

elevated temperatures, while the mixing procedure is less efficient at low temperature series due to a bigger proportion of FR being filled with solidus metallic oxide elements. It results in an increased reaction rate within the reactor at higher temperature ranges. Consequently, it's noted that the rate of fuel conversion increases as the temperature rises. Within this current analysis, the rate of conversion is observed to vary between 0.45 to 0.75 at temperatures 923 K to 1323 K.

An unsteady perturbation of the fraction of mole for gas reactant (CH_4) at interface and reactor outlet at different reactor inlet temperatures of the fuel reactor is presented in Figure 6 (a) and 6 (b) respectively. A simulation was carried out for NiO 0.5 as well as CuO 0.5 by weightage for various temperature ranges: 923 - 1223 K. The fluctuation of gaseous mole fraction within the fuel reactor has been noticed to be more intense at higher temperature ranges.

The proportion of CH_4 moles in the intersection steadily decreases from unity to $t = 2$ s. However, beyond $t = 2$ s, they exhibit irregular fluctuations across all considered temperature ranges. The average molar fraction variation of CH_4 at the outlet decreases progressively from $t = 4$ s for a reactor inlet temperature of 1223 K to $t = 6$ s for a reactor inlet temperature of 923 K. Beyond this point, a quasi-steady distribution of mole fraction is observed. This quasi-periodic variation in CH_4 mole fraction at the outlet may be attributed to the absence of O_2 -carrying elements and less intense reactions.

Figure 7 illustrates the contour depicting the solidus volume fraction across various temperature ranges 923 - 1323 K at a time of 10 seconds. The observation indicates that at elevated temperatures, O_2 transporter molecules are well-mixed with gas-phase fuel particles. In contrast, at relatively lower inlet temperatures, a noticeable presence of metal oxide granules persists within the FR. As a

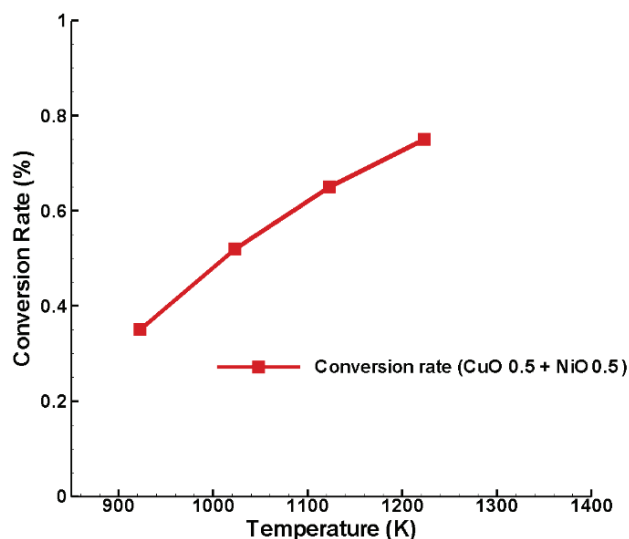


Figure 8. Conversion rates of fuel at outlet for different temperature ranges for 50% CuO and 50% NiO.

consequence, the inter-mixing rate between gas and solid molecules is diminished at lower temperatures, contributing to lower reaction rates.

In Figure 8, the fuel conversion rate outside the reactor is depicted across different temperature ranges. The observation reveals that efficient blending of gas and solidus elements occurs at higher temperatures, whereas the mixing process is less effective at lower temperature series, mainly due to a larger proportion of FR being occupied by solidus metallic oxide elements. This leads to an augmented reaction rate within the reactor at elevated temperature ranges. Consequently, the fuel conversion rate is noted to increase with rising temperatures, ranging from 0.35 to 0.75 in the current analysis at temperatures spanning from 923 K to 1323 K.

Figure 9 presents the dynamic perturbation of the mole fraction for the gas reactant (CH_4) at both the interface and reactor outlet, considering various reactor inlet temperatures for the fuel reactor: NiO 0.3 and CuO 0.7 by weightage. The simulation covers a range of temperatures from 923 K to 1223 K. Notably, the fluctuation in gaseous mole fraction within the fuel reactor is observed to be more pronounced at elevated temperature ranges.

The CH_4 mole fraction at the intersection gradually decreases from unity to $t = 2.5$ s. However, beyond $t = 2.5$ s, it exhibits a highly irregular pattern across all considered temperature ranges. The average molar fraction variation of CH_4 at the outlet decreases progressively, reaching $t = 5$ s for a reactor inlet temperature of 1223 K and $t = 6.5$ s for a reactor inlet temperature of 923 K. Subsequently, a quasi-steady distribution of mole fraction is observed. This quasi-periodic variation in CH_4 mole fraction at the outlet may be attributed to the absence of elements carrying O_2 and less intense reactions.

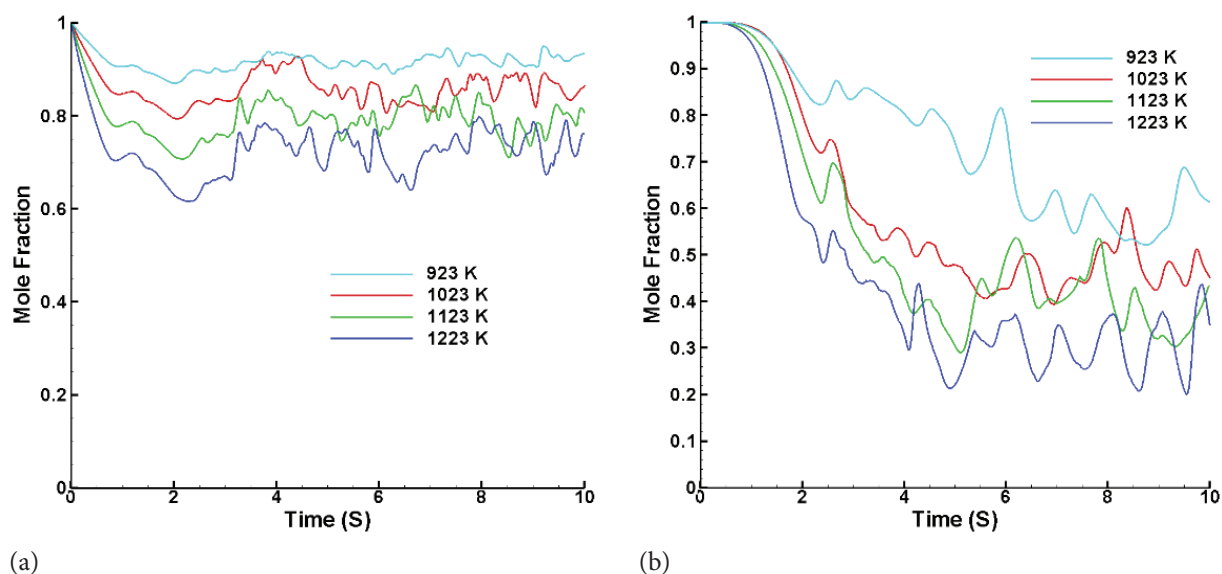


Figure 9. Molar fraction of reactant (CH_4) in (a) intersection and (b) outside for 70% CuO and 30% NiO.

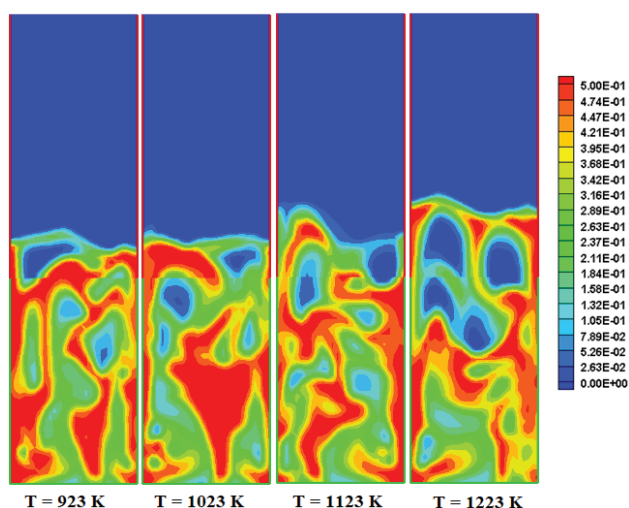


Figure 10. Solid volume fraction contour for various temperatures at time 10 s for 70% CuO and 30% NiO.

Figure 10 illustrates a contour representing the solidus volume fraction across various temperature ranges 923 - 1323 K at a time of 10 seconds. The observation indicates that, at higher temperatures, O_2 transporter molecules are well-integrated within the gas phase fuel particles. In contrast, at relatively lower inlet temperatures, a notable presence of metal oxide granules is still discernible within FR. This disparity leads to a diminished rate of inter-mixing between gas and solid molecules at lower temperatures, resulting in lower response rates.

In Figure 11, the fuel conversion rate outside the reactor is depicted across various temperature series. It is observed that efficient blending of gas and solidus elements occurs at elevated temperatures, while the mixing process is less effective at

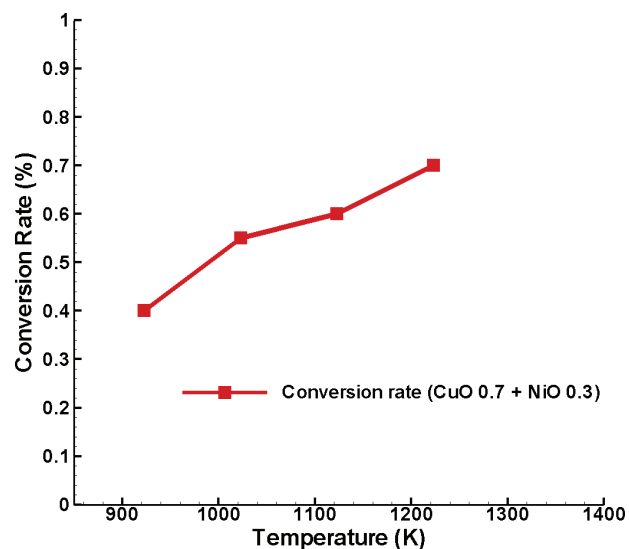


Figure 11. Conversion rates of fuel at outlet for different temperature ranges for 70% CuO and 30% NiO.

lower temperature series, mainly due to a larger proportion of FR being occupied by solidus metallic oxide elements.

This leads to an elevated reaction rate within the reactor at higher temperature ranges. Consequently, it is observed that the rate of fuel conversion increases with rising temperatures. In this current analysis, the conversion rate is noted to vary between 0.40 and 0.70 at temperatures ranging from 923 K to 1323 K.

CONCLUSION

The ANSYS Fluent software was employed to simulate the behavior of gaseous bubbles in the fuel reactor of a CLC

system. In this simulation, the fuel reactor was represented as a fluidized bed reactor initially containing metal oxide granules in the reactor's free-board area. A consistent supply of CH₄ as gaseous fuel was introduced at the reactor's distributor end. The intimate mixing of solid oxygen carrier particles and gaseous fuel facilitated the reaction, resulting in the emergence of gaseous bubbles from the distributor plate. The performance of CLC system has been analyzed for different operating temperatures of fuel reactor. The rate of fuel conversion has increased by increasing the operating temperature for all proportions of mixtures because of the inappropriate mixer of solid and gas particles at a lower temperature. For the NiO 0.7 and CuO 0.3; the rate of conversion is observed to vary between 0.45 to 0.75 at temperatures 923 K to 1323 K. For the NiO 0.5 and CuO 0.5; the rate of conversion is observed to vary between 0.35 to 0.75 at temperatures 923 K to 1323 K. For the NiO 0.3 and CuO 0.7; the rate of conversion is observed to vary between 0.40 to 0.70 at temperatures 923 K to 1323 K. So, the authors would like to suggest using a higher operating temperature to get more fuel conversion rate. The numerical examination of the CLC system can be conducted for various static and freeboard height ranges. The numerical examination of the fuel reactor within a chemical looping combustion system can involve the utilization of various gaseous fuels such as Ethyne, Ethane, Propane, and Butane. The numerical assessment of a CLC system can be conducted by employing solid fuels.

AUTHORSHIP CONTRIBUTIONS

Authors equally contributed to this work.

DATA AVAILABILITY STATEMENT

The authors confirm that the data that supports the findings of this study are available within the article. Raw data that support the finding of this study are available from the corresponding author, upon reasonable request.

CONFLICT OF INTEREST

The authors declared no potential conflicts of interest with respect to the research, authorship, and/or publication of this article.

ETHICS

There are no ethical issues with the publication of this manuscript.

REFERENCES

- [1] Ishida M, Zheng D, Akehata T. Evaluation of a chemical-looping combustion power generation system by graphic energy analysis. *Energy* 1987;12:147–154. [\[CrossRef\]](#)
- [2] Leckner B, Szentannai P, Winter F. Scale-up of fluidized-bed combustion – a review. *Fuel* 2001;90:2951–2964. [\[CrossRef\]](#)
- [3] Lyngfelt A, Leckner B, Mattisson T. A fluidized-bed combustion process with inherent CO₂ separation; application of chemical looping combustion. *Chem Eng Sci* 2001;56:3101–3113. [\[CrossRef\]](#)
- [4] Hossain MM, de Lasa HI. Chemical-looping combustion (CLC) for inherent CO₂ separations—a review. *Chem Eng Sci* 2008;63:4433–4451. [\[CrossRef\]](#)
- [5] Dahl IM, Bakken E, Larring Y, Spjelkavik AI, Hakonsen SF, Blom R. On the development of novel reactor concepts for chemical looping combustion. *Energy Procedia* 2009;1:1513–1519. [\[CrossRef\]](#)
- [6] Kruggel-Emden H, Stepanek F, Munjiza A. A comparative study of reaction models applied for chemical looping combustion. *Chem Eng Res Des* 2011;89:2714–2727. [\[CrossRef\]](#)
- [7] Cho WC, Lee DY, Seo MW. Continuous operation characteristics of chemical looping hydrogen production system. *Appl Energy* 2014;113:1667–1674. [\[CrossRef\]](#)
- [8] Harichandan AB, Shamim T. CFD analysis of bubble hydrodynamics in a fuel reactor for a hydrogen-fueled chemical looping combustion system. *Energy Convers Manag* 2014;86:1010–1022. [\[CrossRef\]](#)
- [9] Harichandan AB, Shamim T. Effect of fuel and oxygen carriers on the hydrodynamics of fuel reactor in a chemical looping combustion system. *J Therm Sci Eng Appl* 2014;6:0410131–0410138. [\[CrossRef\]](#)
- [10] Niu X, Shen L, Gu H, Jiang S, Xiao J. Characteristics of hematite and fly ash during chemical looping combustion of sewage sludge. *Chem Eng J* 2015;268:236–244. [\[CrossRef\]](#)
- [11] Larring Y, Pishahang M, Sunding MF, Tsakalakis K. Fe–Mn based minerals with remarkable redox characteristics for chemical looping combustion. *Fuel* 2015;159:169–178. [\[CrossRef\]](#)
- [12] Khan M, Shamim T. Investigation of hydrogen generation in a three-reactor chemical looping reforming process. *Appl Energy* 2016;162:1186–1194. [\[CrossRef\]](#)
- [13] Yaoyao Z, Grant R, Wenting H, Marek E, Scott SA. H₂ production from partial oxidation of CH₄ by Fe₂O₃-supported Ni-based catalysts in a plasma-assisted packed bed reactor. *Proc Combust Inst* 2019;37:5481–5488. [\[CrossRef\]](#)
- [14] Sedghkerdar MH, Karami D, Mahinpey N. Reduction and oxidation kinetics of solid fuel chemical looping combustion over a core-shell structured nickel-based oxygen carrier: Application of a developed grain size distribution model. *Fuel* 2020;274:117838. [\[CrossRef\]](#)
- [15] Pragadeesh KS, Rugupathi I, Sudhakar DR. In situ gasification – chemical looping combustion of large coal and biomass particles: Char conversion and comminution. *Fuel* 2021;292:120201. [\[CrossRef\]](#)

- [16] Jovanovic R, Marek EJ. Percolation theory applied in modelling of Fe_2O_3 reduction during chemical looping combustion. *Chem Eng J* 2021;406:126845. [CrossRef]
- [17] Liu F, Liu J, Yang Y. Review on the theoretical understanding of oxygen carrier development for chemical-looping technologies. *Energy Fuels* 2022;36:9373–9384. [CrossRef]
- [18] Yamamoto K, Sakaguchi K. Hydrogen reactivity factor and effects of oxygen on methane conversion rate by chemical equilibrium calculation. *Int J Thermofluids* 2022;15:100186. [CrossRef]
- [19] Song Y, Lu Y, Wang M, Liu T, Wang C, Xio R, Zeng D. Screening of natural oxygen carriers for chemical looping combustion based on a machine learning method. *Energy Fuels* 2023;37:3926–3933. [CrossRef]
- [20] Sheth M, Roy A, Harichandan A. Performance of fuel reactor in a chemical looping combustion system with different oxygen carriers. *Therm Sci Eng Prog* 2018;5:303–308. [CrossRef]
- [21] Sheth M, Sigdel S, Harichandan AB, Bhoraniya R. Performance of fuel reactor in chemical looping combustion system with various metal oxide particle size and operating temperature. *Int J Thermofluids* 2023;17:100295. [CrossRef]
- [22] Sheth M, Harichandan AB, Bhoraniya R. Performance of fuel reactor in chemical looping combustion system with mixed metal oxides. *Int J Thermofluids* 2023;20:100524. [CrossRef]
- [23] Mahalatkar K, Kuhlman J, Huckaby ED, O'Brien T. CFD simulation of a chemical-looping fuel reactor utilizing solid fuel. *Chem Eng Sci* 2011;66:3617–3627. [CrossRef]
- [24] Arjmand M, Leion H, Mattisson T, Lyngfelt A. Investigation of different manganese ores as oxygen carriers in chemical-looping combustion (CLC) for solid fuels. *Appl Energy* 2014;113:1883–1894. [CrossRef]
- [25] Vega RP, Abad A, Bueno JA, Garcia-Labiano F, Gayan P, De Diego LF, Adanez J. Improving the efficiency of chemical looping combustion with coal by using ring-type internals in the fuel reactor. *Fuel* 2019;250:8–16. [CrossRef]
- [26] Adanez J, Gayan P, De Diego LF, Garcia-Labiano F, Abad A. Combustion of wood chips in a CFBC. Modeling and validation. *Ind Eng Chem Res* 2003;42:987–999. [CrossRef]
- [27] Jung J, Gamwo IK. Multiphase CFD-based models for chemical looping combustion process: Fuel reactor modeling. *Powder Technol* 2008;183:401–409. [CrossRef]
- [28] Khongprom P, Gidaspow D. Compact fluidized bed sorber for CO_2 capture. *Particuology* 2010;8:531–535. [CrossRef]
- [29] Xiao R, Song Q. Characterization and kinetics of reduction of CaSO_4 with carbon monoxide for chemical-looping combustion. *Combust Flame* 2011;158:2524–2539. [CrossRef]
- [30] Snider DM, Clark SM, O'Rourke PJ. Eulerian–Lagrangian method for three-dimensional thermal reacting flow with application to coal gasifiers. *Chem Eng Sci* 2011;66:1285–1295. [CrossRef]
- [31] Gayan P, Forero CR, Abad A, De Diego LF, Labiano FG, Adanez J. Effect of support on the behaviour of Cu-based oxygen carriers during long-term CLC operation at temperatures above 1073 K. *Energy Fuels* 2011;25:1316–1326. [CrossRef]
- [32] Rajak U, Nashine P, Chaurasiya P, Verma T. A numerical investigation of the species transport approach for modeling of gaseous combustion. *J Therm Eng* 2021;7:2054–2067. [CrossRef]
- [33] Deng Z, Xiao R, Jin B, Song Q. Numerical simulation of chemical looping combustion process with CaSO_4 oxygen carrier. *Int J Greenh Gas Control* 2009;3:368–375. [CrossRef]
- [34] Gelderbloom SJ, Gidaspow D, Lyczkowski RW. CFD simulations of bubbling/collapsing fluidized beds for three Geldart groups. *AIChE J* 2003;49:844–858. [CrossRef]
- [35] Clift R, Grace JR. *Continuous Bubbling and Slugging*. London: Academic Press; 1985.